Three-dimensional instability of Kirchhoff's elliptic vortex : Its relation to the elliptical instability(Mathematical Fluid Mechanics and Modeling)

AUTHOR(S):

Miyazaki, Takeshi; Fukumoto, Yasuhide

数理解析研究所講究録
第888巻 1994年 96-111

Three-dimensional instability of Kirchhoff's elliptic vortex
- Its relation to the elliptical instability -

Univ. Electro-Communications Takeshi Miyazaki (宮嵜 武)
Nagoya Univ. Yasuhide Fukumoto (福本康秀)

1. Introduction

The three-dimensional instability modes of concentrated vortices are classified into two categories according to their axial wavelengths. One with the longer wavelength (much longer than the vortex core radius) is called the Crow instability[1], which explains the destabilization of trailing vortices shed from an aircraft. Tsai & Widnall[2] and Moore & Saffman[3] found that a columnar vortex embedded in a strain field is unstable to the bending perturbations whose axial wavelength is order of the core radius. Widnall, Bliss & Tsai[4] succeeded in explaining the destabilization of a vortex ring following the same lines of consideration.

Recently, Pierrehumbert[5] showed numerically that an unbounded inviscid strained vortex undergoes instability whose growth rate is independent of wavelength. Bayly[6] formulated the problem as a matrix Floquet problem, which suggested that the instability is prametrically excited. It is, by now, recognized that the Floquet-mechanism is the essence of the short-wave instabilities. Waleffe[7] gave, in the limiting case of weak strain, a clear physical explanation of the instability as a resonant interaction between the inertial wave and the imposed strain field. These instabilities are called the elliptical instability, since they are induced whenever streamlines of a basic flow endowed with vorticity are deformed elliptically. It is not difficult to incorporate the viscous effect, which was undertaken by Landman and Saffman[8]. They showed that this intrinsically inviscid instability mechanism persists even in the presence of the viscous dissipation. Craik[9] proposed to incorporate the contribution of various types of body force and described the influence of a Coriolis force in detail. Miyazaki & Fukumoto[10] addressed a

question of the effect of a buoyancy force and Miyazaki[11] considered the combined effect of both forces on the elliptical instability.

In spite of the abundance of studies on the elliptical instability, the relevance of the mechanism to the actual flow fields is not fully understood. Gledzer and Ponomarev[12] investigated the instability of a solid body rotation of fluid in an elliptical cylinder and compared their results with the predictions of the elliptical instability. The numerical investigations[13-15] of Poiseuille flows have revealed that finite-amplitude two-dimensional waves are unstable to short-wave three-dimensional instabilities. It is considered that the continuous instabilities are discritized to form an infinite number of separate short-wave instability bands, if an appropriate outer boundary condition is taken into account[16]. Our objective in this paper is to manifest the broad generality of the elliptical instability by investigating numerically the linear instability of an elliptic vortex patch of finite extent. Pierrehumbert & Widnall[17] investigated the linear stability of the Stuart vortex and Robinson & Saffman[18] considered the Moore-Saffman vortex[19], before the birth of the concept of elliptical instability. Our work will serve to complement these precursors.

Specifically, we focus our attention on Kirchhoff's elliptic vortex, a vortex patch with uniform vorticity ω_0 inside of an ellipse whose major and minor semi-axes are a and b. If it is embedded in an irrotational fluid, it rotates solidly with a constant angular velocity $\Omega=\omega_0 ab/(a+b)^2$. A century ago, Love[20] studied the two-dimensional linear instability of the Kirchhoff's elliptic vortex and found that it becomes unstable to disturbances with azimuthal wave number 3, if the ratio a/b is greater than 3. As for the three-dimensional stability, Vladimirov & Il'in[21] made an asymptotic analysis in the limit of small eccentricity, and showed that there are infinite number of instability bands. Our numerical analysis extends their results to the case of finite ellipticity.

2. Formulation

2.1 Kirchhoff's elliptic vortex

Let us assume that the fluid is inviscid and incompressible. The streamfunction (in the inertial frame) inside of Kirchhoff's elliptic vortex is given by[20],

$$\Psi_{in}^{(i)} = -\frac{bx^2+ay^2}{2(a+b)}, \qquad (1)$$

where the uniform vorticity ω_0 in the interior of the ellipse is taken to be unity and a is the major semi-axis and b is the minor semi-axis. The elliptic vortex rotates rigidly about the z-axis with a constant angular velocity

$$\Omega = \frac{ab}{(a+b)^2}. \qquad (2)$$

Hence, the ellipse is stationary if we move into the coordinate frame rotating with the angular velocity Ω around the z-axis. The (rotating) Cartesian coordinates (x, y, z) are used, hereafter, with the corresponding unit vectors e_x, e_y and e_z. The streamfunction (1) in the inertial frame is augmented by a collection term as,

$$\Psi_{in} = -\frac{bx^2+ay^2}{2(a+b)} + \frac{1}{2}\Omega\,(x^2+y^2). \qquad (1')$$

It is noted that the interior vorticity is reduced to $\omega'_0=(a^2+b^2)/(a+b)^2$ in the rotating coordinates. The use of the elliptic-cylinder coordinates (ξ, η, z) is convenient in describing the geometry of the basic flow field:

$$x = c\cosh\xi\cos\eta, \qquad (3a)$$

$$y = c\sinh\xi\sin\eta, \quad 0\le\eta\le 2\pi, \qquad (3b)$$

where $c=\sqrt{a^2-b^2}$ and h^2 denotes the metric factor:

$$h^2 = \frac{1}{2}c^2(\cosh 2\xi - \cos 2\eta). \qquad (3c)$$

In these coordinates, the boundary of the ellipse is represented by

$$\xi = \xi_0 = \frac{1}{2}\log\left(\frac{a+b}{a-b}\right), \qquad (4)$$

and the streamfunction outside of the vortex is written as

$$\Psi_{out} = -\frac{ab}{2}\xi - \frac{ab}{4}e^{-2\xi}\cos 2\eta + \frac{1}{2}\Omega\,(x^2+y^2). \qquad (5)$$

2.2 Perturbation equations

Since the basic flow is uniform in the z-direction, we can introduce the normal-mode disturbances of small amplitude with the form proportional to $e^{i(kz-\omega t)}$, where k is the axial wavenumber:

$$
\begin{aligned}
u_\xi^{in} &= U_\xi^{in} + \bar{\varepsilon}\, u_\xi\, e^{i(kz - \omega t)},\\
u_\eta^{in} &= U_\eta^{in} + \bar{\varepsilon}\, u_\eta\, e^{i(kz - \omega t)},\\
w^{in} &= \bar{\varepsilon}\, \bar{w}\, e^{i(kz - \omega t)},\\
p^{in} &= P^{in} + \bar{\varepsilon}\, \bar{p}\, e^{i(kz - \omega t)},
\end{aligned}
\tag{6}
$$

where $\bar{\varepsilon}$ is a small parameter ($\bar{\varepsilon}<<1$). Since the flow is irrotational outside of the ellipse, we may assume that the disturbances are irrotational, too, there:

$$
\begin{aligned}
u_\xi^{out} &= U_\xi^{out} + \bar{\varepsilon}\, \frac{\partial \bar{\phi}}{h\partial\xi}\, e^{i(kz - \omega t)},\\
u_\eta^{out} &= U_\eta^{out} + \bar{\varepsilon}\, \frac{\partial \bar{\phi}}{h\partial\eta}\, e^{i(kz - \omega t)},\\
w^{out} &= W^{out} + \bar{\varepsilon}\, ik\bar{\phi}\, e^{i(kz - \omega t)}.
\end{aligned}
\tag{7}
$$

The linearized Eulerian equations of motion in the elliptic-cylinder coordinates are

$$
\begin{aligned}
&-i\omega\bar{u} + \frac{1}{h^2}\left[\bar{U}\frac{\partial}{\partial\xi} + \bar{V}\frac{\partial}{\partial\eta}\right]\bar{u} + \frac{1}{h^2}\left[\bar{u}\frac{\partial}{\partial\xi} + \bar{v}\frac{\partial}{\partial\eta}\right]\bar{U}\\
&\quad + (\bar{U}\,\bar{u} + \bar{V}\,\bar{v})\,\frac{\partial}{\partial\xi}\left(\frac{1}{h^2}\right) - 2\Omega\bar{v} = -\frac{\partial\bar{p}}{\partial\xi},
\end{aligned}
\tag{8a}
$$

$$
\begin{aligned}
&-i\omega\bar{v} + \frac{1}{h^2}\left[\bar{U}\frac{\partial}{\partial\xi} + \bar{V}\frac{\partial}{\partial\eta}\right]\bar{v} + \frac{1}{h^2}\left[\bar{u}\frac{\partial}{\partial\xi} + \bar{v}\frac{\partial}{\partial\eta}\right]\bar{V}\\
&\quad + (\bar{U}\,\bar{u} + \bar{V}\,\bar{v})\,\frac{\partial}{\partial\eta}\left(\frac{1}{h^2}\right) + 2\Omega\bar{u} = -\frac{\partial\bar{p}}{\partial\eta},
\end{aligned}
\tag{8b}
$$

$$
-i\omega\bar{w} + \frac{1}{h^2}\left[\bar{U}\frac{\partial}{\partial\xi} + \bar{V}\frac{\partial}{\partial\eta}\right]\bar{w} = -ik\bar{p},
\tag{8c}
$$

$$
\frac{1}{h^2}\left(\frac{\partial\bar{u}}{\partial\xi} + \frac{\partial\bar{v}}{\partial\eta}\right) + ik\bar{w} = 0,
\tag{9}
$$

where new dependent variables $\bar{u} = hu_\xi$ and $\bar{v} = hu_\eta$ with $\bar{U} = hU_\xi^{in}$ and $\bar{V} = hV_\xi^{in}$ are introduced. Note that the Coriolis terms proportional to 2Ω are added to those given by Robinson & Saffman[18]. Eliminating $\bar{w}$ and $\bar{p}$ using the continuity equation (9) and the third component of the Eulereian equation (8c), we are left with coupled equations for $\bar{u}$ and $\bar{v}$:

$$- i\omega \{\bar{u} - \frac{1}{k^2}\frac{\partial}{\partial\xi}[\frac{1}{h^2}(\frac{\partial\bar{u}}{\partial\xi} + \frac{\partial\bar{v}}{\partial\eta})]\} = -\frac{1}{h^2}(\bar{U}\frac{\partial}{\partial\xi} + \bar{V}\frac{\partial}{\partial\eta})\bar{u} - \frac{1}{h^2}(\bar{u}\frac{\partial}{\partial\xi} + \bar{v}\frac{\partial}{\partial\eta})\bar{U}$$
$$- (\bar{U}\bar{u} + \bar{V}\bar{v})\frac{\partial}{\partial\xi}(\frac{1}{h^2}) + 2\Omega\bar{v} + \frac{1}{k^2}\frac{\partial}{\partial\xi}\{\frac{1}{h^2}(\bar{U}\frac{\partial}{\partial\xi} + \bar{V}\frac{\partial}{\partial\eta})[\frac{1}{h^2}(\frac{\partial\bar{u}}{\partial\xi} + \frac{\partial\bar{v}}{\partial\eta})]\}$$

$$- i\omega \{\bar{v} - \frac{1}{k^2}\frac{\partial}{\partial\eta}[\frac{1}{h^2}(\frac{\partial\bar{u}}{\partial\xi} + \frac{\partial\bar{v}}{\partial\eta})]\} = -\frac{1}{h^2}(\bar{U}\frac{\partial}{\partial\xi} + \bar{V}\frac{\partial}{\partial\eta})\bar{v} - \frac{1}{h^2}(\bar{u}\frac{\partial}{\partial\xi} + \bar{v}\frac{\partial}{\partial\eta})\bar{V}$$
$$- (\bar{U}\bar{u} + \bar{V}\bar{v})\frac{\partial}{\partial\eta}(\frac{1}{h^2}) - 2\Omega\bar{u} + \frac{1}{k^2}\frac{\partial}{\partial\eta}\{\frac{1}{h^2}(\bar{U}\frac{\partial}{\partial\xi} + \bar{V}\frac{\partial}{\partial\eta})[\frac{1}{h^2}(\frac{\partial\bar{u}}{\partial\xi} + \frac{\partial\bar{v}}{\partial\eta})]\}$$
(10a,b)

Since these equations (10a,b) are singular at h=0, they are multiplied by h^8 in implementing the numerical procedure below.

The potential $\bar{\phi}(\xi, \eta)$ outside of the vortex obeys the Helmholtz equation:

$$[\frac{\partial^2}{\partial\xi^2} + \frac{\partial^2}{\partial\eta^2} - 2q(\cosh 2\xi - \cos 2\eta)]\,\bar{\phi} = 0, \qquad (11)$$

with $q = \frac{1}{4}c^2k^2$. Equation (11) is separable and the solution is obtainable in the form of expansions in terms of the Mathieu functions.

The boundary of the vortex patch is assumed to deform as

$$\xi = \xi_0 + \bar{\varepsilon}\,F(\eta)e^{i(kz - \omega t)}. \qquad (12)$$

At $O(\bar{\varepsilon})$, the kinematical boundary conditions that the boundary of the vortex patch continues to be the boundary are written, on $\xi=\xi_0$, as

$$i\omega h^2 F + \bar{u} - \Omega\frac{\partial}{\partial\eta}(h^2 F) = 0, \qquad (13a)$$

$$i\omega h^2 F + \frac{\partial\bar{\phi}}{\partial\xi} - \Omega\frac{\partial}{\partial\eta}(h^2 F) = 0. \qquad (13b)$$

The dynamical conditions on $\xi=\xi_0$ require the continuity of tangential velocity components, which are equivalent to the condition of pressure continuity:

$$\frac{\partial\bar{\phi}}{\partial\eta} - \bar{v} = h^2 F, \qquad (14a)$$

$$\frac{\partial^2\bar{\phi}}{\partial\xi^2} - \frac{\partial\bar{u}}{\partial\xi} = -\frac{\partial}{\partial\eta}(h^2 F). \qquad (14b)$$

2.3 Numerical procedure

Since the formulation of numerical eigenvalue problems is essentially identical to those of Robinson & Saffman[18], we will give only a brief outline. The velocity components $\bar{u}$ and $\bar{v}$ inside of the vortex are expanded (doubly) in terms of the Mathieu-Tchebyscheff functions, as

$$\bar{u}^{o} = \sum_{m=1}^{\infty}\sum_{n=1}^{\infty}\left[C^{u}_{mn} ce_{2m-1}(\eta,-q)\, T_{2n-1}\left(\frac{\xi}{\xi_0}\right) + D^{u}_{mn} se_{2m-1}(\eta,-q)\, T_{2n-2}\left(\frac{\xi}{\xi_0}\right)\right], \tag{15a}$$

$$\bar{v}^{o} = \sum_{m=1}^{\infty}\sum_{n=1}^{\infty}\left[C^{v}_{mn} ce_{2m-1}(\eta,-q)\, T_{2n-1}\left(\frac{\xi}{\xi_0}\right) + D^{v}_{mn} se_{2m-1}(\eta,-q)\, T_{2n-2}\left(\frac{\xi}{\xi_0}\right)\right], \tag{15b}$$

where the superscript o denotes that the function is 2π-periodic (odd) with respect to the variable η. They are decoupled from the π-periodic (even) modes, because the basic flow (Kirchhoff's elliptic vortex) is π-periodic in η. In this paper, we confine our attention to the odd modes, which have the same symmetry-nature with the elliptical instability. The functions ce and se denote the Mathieu functions. The coefficients of the outer Mathieu-expansions can be expressed using C^{u}_{mn} and D^{u}_{mn} and the problem is reduced to a smaller eigenvalue problem. To see this, we notice from (13a) and (13b) that the following relation is satisfied at the vortex boundary:

$$\bar{u} = \frac{\partial \bar{\phi}}{\partial \xi}. \tag{16}$$

The outer potential is then expressed as,

$$\bar{\phi} = \sum_{m=1}^{\infty}\sum_{n=1}^{\infty}\left[C^{u}_{mn} ce_{2m-1}(\eta,-q)\frac{Ke_{2m-1}(\xi, q)}{Ke_{2m-1}(\xi_0, q)} + D^{u}_{mn} se_{2m-1}(\eta,-q)\frac{Ko_{2m-1}(\xi, q)}{Ko_{2m-1}(\xi_0, q)}\right], \tag{17}$$

where Ke and Ko are the modified Mathieu functions (see e.g. Abramowitz & Stegun[23]). The characteristic values and the functional values of the Mathieu functions are computed using appropriate routines and their modifications. The functional values of the modified Mathieu functions Ke and Ko are available

by integrating the governing equation numerically (see, for details, Robinson & Saffman[18]).

We require that the interior equations (10a) and (10b), with the factor h^8 multiplied, are satisfied at the collocation points, where

$$\frac{\xi_i}{\xi_0} = \cos\frac{\pi\,(2i-1)}{4\,(N_R-1)}, \quad i = 1,2,\ldots N_R - 1,$$
$$\eta_j = \frac{\pi\,(j-1)}{2\,N_A}, \qquad j = 1,2,\ldots 2N_A. \tag{18}$$

The boundary conditions (13) and (14) are cast into,

$$-i\omega\left(\frac{\partial\bar{\phi}}{\partial\eta} - \bar{v}\right) = \bar{u} + \Omega\left(\frac{\partial^2\bar{u}}{\partial\xi^2} - \frac{\partial\bar{u}}{\partial\xi}\right), \tag{19a}$$

$$0 = \frac{\partial\bar{u}}{\partial\xi} + \frac{\partial\bar{v}}{\partial\eta} - k^2h^2\bar{\phi}, \tag{19b}$$

which are to be satisfied at

$$\xi = \xi_0,\ \eta_j = \frac{\pi\,(j-1)}{2\,N_A},\ j = 1,2,\ldots 2N_A. \tag{20}$$

Truncating the expansions at a finite order $n=N_R$ and $m=N_A$, we obtain the following matrix-type relation:

$$-i\omega\,\mathbf{A}\begin{pmatrix} C^u_{mn} \\ D^u_{mn} \\ C^v_{mn} \\ D^v_{mn} \end{pmatrix} = \mathbf{B}\begin{pmatrix} C^u_{mn} \\ D^u_{mn} \\ C^v_{mn} \\ D^v_{mn} \end{pmatrix}. \tag{21}$$

Here, **A** and **B** are $4N_RN_A \times 4N_RN_A$ matrices. The matrix **A** is singular, i.e., the last $2N_A$ rows (corresponding to (19b)) are zero, whereas the matrix **B** is regular. The eigenvalues i/ω of the matrix $\mathbf{AB}^{-1}$ ($4N_RN_A \times 4N_RN_A$) are calculated numerically using the QR method. We notice that the matrix has $2N_A$ zero-eigenvalues, so we have to calculate the eigenvalues of a $4(N_R-1/2)N_A \times 4(N_R-1/2)N_A$ matrix. The truncation numbers N_R and N_A, which are typically 12, are increased up to 15 separately when it is necessary to achieve the accuracy of four significant figures.

3. Results

We show in Figs. 1a-c, the calculated growth rate of the three-dimensional instability for the cases of a/b=1.1, 2.0 and 3.0, respectively. The horizontal axis is the axial wavenumber k (here, the length-scale is normalized by *b*) and the vertical axis is the

imaginary part of ω (σ=Im(ω)). The instability is not oscillatory, since the calculated ω is pure imaginary whenever it has a nonzero imaginary part. Love's two-dimensional result[20] tells that an ellipse whose a/b is less than 3, is stable against any two-dimensional (k=0) disturbances, which is confirmed from the figures. It follows that Kirchhoff's elliptic vortex of a/b<3 is free from the long wave instabilities in contrast with the Moore-Saffman vortex[18,19].

In Fig.1a, we recognize three instability bands centered at k_1=1.0, k_2=1.8 and k_3=2.6. It is noteworthy that the maximum growth rate ($\sigma_{1,2,3}$=0.0094) of each mode is common. The location of the instability band is close to the value obtained by Vladimirov and Il'in[21] in the limit of small ellipticity, i.e., k_1=1.0350, k_2=1.8655 and k_3=2.6844. The values of growth rate are not far from the values estimated from their results, i.e., σ_1=0.00993, σ_2=0.01001 and σ_3=0.01006, also. As a/b increases, both the number (k<3) and the growth rate of instability band increase. We see 5-6 instability bands in Fig.1b (a/b=2.0) and 6-8 bands in Fig.1c (a/b=3.0). It will be natural to think, from these observations, that there are an infinite number of instability modes. Every instability band becomes fatter with a/b and the neighboring bands overlap to form continuos band of almost constant growth rate. Moreover, as is evident from the fact that the interval spacing of bands decreases and band width increases with k, the continuous broad instability band will exist for large values of k, even for the small values of a/b. We show the obtained numerical values in Table 1. The maximum growth rate of each band is the same, except for that of the longest mode which has a slightly larger growth rate. In the last low of Table 1, we listed the growth rate of the elliptical instability (see the next section for details). We notice remarkable coincidence between our numerical values and the predictions of the elliptical instability.

We show, as a contour map in the x-y plane, the distributions of the axial velocity of the lowest eigenmode (k=0.42: Fig.2a) and of the second eigenmode (k=1.0: Fig.2b) for a/b=3.0. The azimuthal wavenumber m is 1 inside of the ellipse in both figures. One node line is added in Fig. 2b. It is likely that the internal structure

becomes more complex as the axial wavenumber of the instability mode increases and that the ith mode has i-1 node lines inside of the ellipse. These figures have resemblance with those of Pierrehumbert[5] (Fig.2) and of Waleffe[7] (Fig.2), indicating the intimate relation to the elliptical instability even at lower modes. In Fig.2a, we observe the azimuthal dependence of m=3 outside of the ellipse, which disappears in Fig.2b, completely. It may provide a possible explanation why the growth rate of the lowest instability mode is slightly greater than those of higher modes. In contrast, very small axial velocity, whose azimuthal dependence is characterized by the wavenumber m=1, is found outside of the vortex in Fig.2b. The higher modes (i > 2) are thought to be confined in the interior of the ellipse, similarly.

4. Relation to the elliptical instability

The numerical results in the previous section demonstrate that the elliptical instability does play a crucial role in the destabilization of a vortex patch of finite extent. The aim of this section is to give a physical interpretation of the theoretical (asymptotic) results of Vladimirov & Il'in[21] and Tsai & Widnall[2] and the numerical results of Robinson & Saffman[18], from this stand point.

First, we describe the derivation of the values in the last row of Table1, which are estimated by the local analysis for the elliptical instability influenced by a Coriolis force. In the rotating coordinates, the vorticity inside of the ellipse is reduced to $\omega'_0=(a^2+b^2)/(a+b)^2$ and the Rossby number (Miyazaki[11] used the inverse of the usual definition) is $4ab/(a^2+b^2)$. The prescription for the determination of the Floquet exponents is found in Craik[9] and Miyazaki[11]. We show the results in Fig.3. The horizontal axis is the angle θ between the initial wavenumber vector and the z-axis. The vertical axis is the growth rate σ of the instability. Seven cases (a/b=1.5, 2.0, 3.0, 4.0, 5.0 , 6.0 and 7.0) are figured by seven lines of different type. As a/b is increased, the instability band width increases and so is the maximum growth rate. The latter, however, saturates and tend to decrease if a/b is increased over about 5.0. The numerical values listed in the bottom of Table1 are calculated in this way. It is interesting to note that the value $\theta=0.3725\pi$,

where the maximum is attained for a/b=3.0, has a close relation to the axial velocity profiles in Fig.2b. If we approximate the profile by $J_1(\kappa\rho)$ ($\rho=(x^2/9+y^2)^{1/2}$: following Waleffe), κ is estimated to be about 6.9 from the fact that the first zero of the Bessel function is $\kappa\rho=3.83$, which corresponds to $\rho=0.55$ in the figure. The value of μ in Waleffe[7] is equal to k(=1.0). Remembering the definition $\tan\theta=\kappa/3\mu$, we have $\theta=0.37\pi$, which is close to the above value. This observation provides another evidence that our numerical results are closely linked to the elliptical instability.

We plot the maximum growth rate against a/b in Fig.4, where Love's two-dimensional result[20] is included for comparison. It can be seen that for ellipses with a/b less than about 3.5, the three-dimensional elliptical instability pre-dominates over the two-dimensional instability.

Next, we will revisit the results of Robinson & Saffman[18], who investigated the instability of an elliptical vortex subject to a uniform strain. They found, besides the long-wave mode, short-wave instability bands, of which two modes were figured in their Fig.3. The maximum growth rate of the two modes is the same in the graphical accuracy and can be read as $\sigma_{1i}=0.104$ (i=1,2) for a/b=1.5 and $\sigma_{1i}=0.153$ (i=1,2) for a/b=2.0. These values are compared with the predictions of the elliptical instability, i.e., $\sigma=0.1046$ for a/b=1.5 and $\sigma=0.1530$ for a/b=2.0. We notice the remarkable coincidence, again. Only the first short-wave mode is shown in their Fig.10, whose maximum growth rate is read to be $\sigma_{11}=0.180$ for a/b=4.0. It is greater than the estimate $\sigma=0.1713$ of the elliptical instability. The same is true of the longest instability mode of Kirchhoff's ellipse. The reason for this phenomena is that the lowest mode is likely to suffer the influence of two-dimensional instabilities, which become dominant as a/b is increased. We draw, in Fig.5, the growth rate of the elliptical instability (Pierrehumbert[5] and Bayly[6]) as a function of a/b together with the growth rate of the two-dimensional instability (m=2: Moore & Saffman[19]). The Moore-Saffman ellipse with a/b less than about 3.9 is more susceptible to the three-dimensional elliptical instability than to the two-dimensional instability.

Finally, we compare the theoretical results of Tsai & Widnall[2] and Vladimirov & Il'in[21], which are based on the asymptotic

calculation in the limit of small ellipticity, with the prediction of the elliptical instability. Waleffe[7] deduced that the growth rate of the elliptical instability asymptotes to $9/16\varepsilon=0.5625\varepsilon$ for $\varepsilon=a/b-1<<1$. This value is close to the results of Tsai & Widnall[2], who determined the growth rate of the lowest mode to be 0.5708ε and that of the second mode to be 0.5695ε. Similarly, the elliptical instability under the influence of a Coriolis force yields the asymptotic growth rate of $[\omega'_0(2R_0+3)^2/32(R_0+1)^2]\varepsilon$, where ω'_0 is the vorticity inside of the ellipse viewed from the rotating coordinate frame and R_0 denotes the Rossby number. Remembering that $\Omega=1/4$ in the limit of a/b--->1, we have $\omega'_0=1-2(1/4)=1/2$, $R_0=(1/4)/(\omega'_0/2)=1$ and then the growth rate $25/256\varepsilon=0.0977\varepsilon$. It again approximates the values 0.993ε, 0.1001ε, 0.1005ε, 0.1009ε and 0.1012ε obtained by Vladimirov & Il'in[21] (note that their definition of the parameter ε is different from ours by a factor 2). Even in this limiting case, the elliptical instability does a good job.

The two vortex patches of finite extent considered here, i.e., Kirchhff's ellipse and the Moore-Saffman elliptic vortex are embedded in an irrotational fluid. No source of instability is presented outside of the patches, if it were not for stagnation points. Our findings demonstrate that the estimate based on the concept of the elliptical instability gives quite accurate predictions of the instability growth rate (within a few percent), at least, in these cases. More stringent check will be provided if we investigate the three-dimensional linear instability of general Moore-Saffman vortices[19] embedded in a uniform background vorticity field. In this case, possible instability sources are presented both inside and outside of the ellipse.

5. Summary and discussions

We have investigated the three-dimensional linear instability of Kirchhoff's elliptic vortex. Any ellipse, irrespective of the ratio a/b(=semi-major axis/semi-minor axis), is shown to be unstable to the m=1 bending mode. There are an infinite number of instability bands, whose locations in the limit of small ellipticity coincide with the asymptotic results by Vladimirov & Il'in[21]. The width of instability band broadens and the neighboring bands overlap, as

a/b and the axial wavenumber k increase. The maximum growth rate of each band (except for that of the lowest mode) is estimated by the prediction based on the elliptical instability accurately. The structure of eigenmode in the x-y plane becomes more complex as the axial wavenumber increases (for the i-th mode, i-1 node lines are presented inside of the ellipse). The profile of the axial velocity (especially, near the center of the vortex) resembles that of the elliptical instability. This mechanism predominates over the two-dimensional instability for smaller values of a/b.

We have reconsidered both the asymptotic results of Tsai & Widnall[2] and Vladimirov & Il'in[21] and the numerical results of Robinson & Saffman[18], from the standpoint of the elliptical instability. In every case, the values of the instability growth rate obtained in the earlier studies are close to the values predicted by the elliptical instability.

We speculate through these observations that the concept of the elliptical instability is quite useful in estimating the strength of three-dimensional bending instabilities of steady isolated columnar vortices, even of finite extent. Since the growth rate of the linear instability is almost independent of the axial wavelength, the breaking process of Kirchhoff's elliptic vortex and the Moore-Saffman vortex will be highly sensitive to initial conditions and/or external noises.

a/b \ n	1. 1		2. 0		3. 0	
	σ	k	σ	k	σ	k
1	0. 0094	1. 0	0. 062	0. 7	0. 089	0. 4
2	0. 0094	1. 8	0. 061	1. 3	0. 083	1. 0
3	0. 0094	2. 6	0. 061	1. 8	0. 082	1. 4
4			0. 061	2. 4	0. 082	1. 9
5			0. 061	3. 0	0. 082	2. 4
6					0. 082	2. 8
∞	0. 0093	∞	0. 0602912	∞	0. 0809604	∞

Table1 The maximum growth rate of each instability band. The values predicted by the elliptical instability (n, k $\longrightarrow \infty$) are listed in the last row.

References

[1]S.C. Crow, "Stability theory for a pair of trailing vortices," *AIAA J.* **8**, 2172 (1970).

[2]C.Y. Tsai and S.E. Widnall, "The stability of short waves on a straight vortex filament in a weak externally imposed strain field," *J. Fluid Mech.* **73**, 721 (1976).

[3]D.W. Moore and P.G. Saffman, "The instability of a straight vortex filament in a strain field," *Proc. R. Soc. London Ser.* **A346**, 415 (1975).

[4]S.E. Widnall, D.B. Bliss and C.Y. Tsai, "The instability of short waves on a vortex ring," *J. Fluid Mech.* **66**, 35 (1974).

[5]R.T. Pierrehumbert, "Universal short-wave instability of two-dimensional eddies in an inviscid fluid," *Phys. Rev. Lett.* **57**, 2157 (1986).

[6]B.J. Bayly, "Three-dimensional instability of elliptical flow," *Phys. Rev. Lett.* **57**, 2160 (1986).

[7]F. Waleffe, "On the three-dimensional instability of strained vortices," *Phys. Fluids* **A2**, 76 (1990).

[8]M.J. Landman and P.G. Saffman, "The three-dimensional instability of strained vortices in a viscous fluid," *Phys. Fluids* **30**, 2339 (1987).

[9]A.D.D. Craik, "The stability of unbounded two- and three- dimensional flows subject to body forces: some exact solutions," *J. Fluid Mech.* **198**, 275 (1989).

[10]T. Miyazaki and Y. Fukumoto, "Three-dimensional instability of strained vortices in a stably stratified fluid," *Phys. Fluids* **A4**, 2515 (1992).

[11]T. Miyazaki, "Elliptical instability in a stably stratified rotating fluid," *Phys. Fluids* **A5**, 2702 (1993).

[12]E.B. Gledzer and V.M. Ponomarev, "Instability of bounded flows with elliptical streamlines," *J. Fluid Mech.* **240**, 1 (1992).

[13]S.A. Orszag and A. Patera, "Secondary instability of wall-bounded shear flows," *J. Fluid Mech.* **128**, 347 (1983).

[14]T. Herbert, "Secondary instability of plane channel flow to subharmonic three-dimensional disturbances," *Phys. Fluids* **26**, 871 (1983).

[15]B.J. Bayly, S.A. Orszag and T. Herbert, "Instability mechanisms in shear-flow transitions," *Annu. Rev. Fluid Mech.* **20**, 359 (1988).

[16]Malkus and F. Waleffe, "Transition from order to disorder in elliptical flow: a direct path to shear flow turbulence," *Advances in Turbulence* **3** (Proc. 3rd European Turb. Conf.), Springer, 197 (1991).

[17]R.T. Pierrehumbert and S.E. Widnall, "The two- and three-dimensional instabilities of a spatially periodic shear layer," *J. Fluid Mech.* **114**, 59 (1982).

[18]A.C. Robinson and P.G. Saffman, "Three-dimensional stability of an elliptical vortex in a straining field," *J. Fluid Mech.* **142**, 451 (1984).

[19]D.W. Moore and P.G. Saffman, "Structure of a line vortex in an imposed strain," in *Aircraft Wake Turbulence* (ed. Olsen, Goldburg & Rogers, Plenum, 1971), p. 399.

[20]A.E.H. Love, "On the stability of certain vortex motions," Proc. London Math. Soc. **25**, 18 (1893).

[21]V.A. Vladimirov and K.I. Il'in, "Three-dimensional instability of an elliptic Kirchhoff vortex," *Mech. Zhid. i Gaza* **3**, 40 (1988).

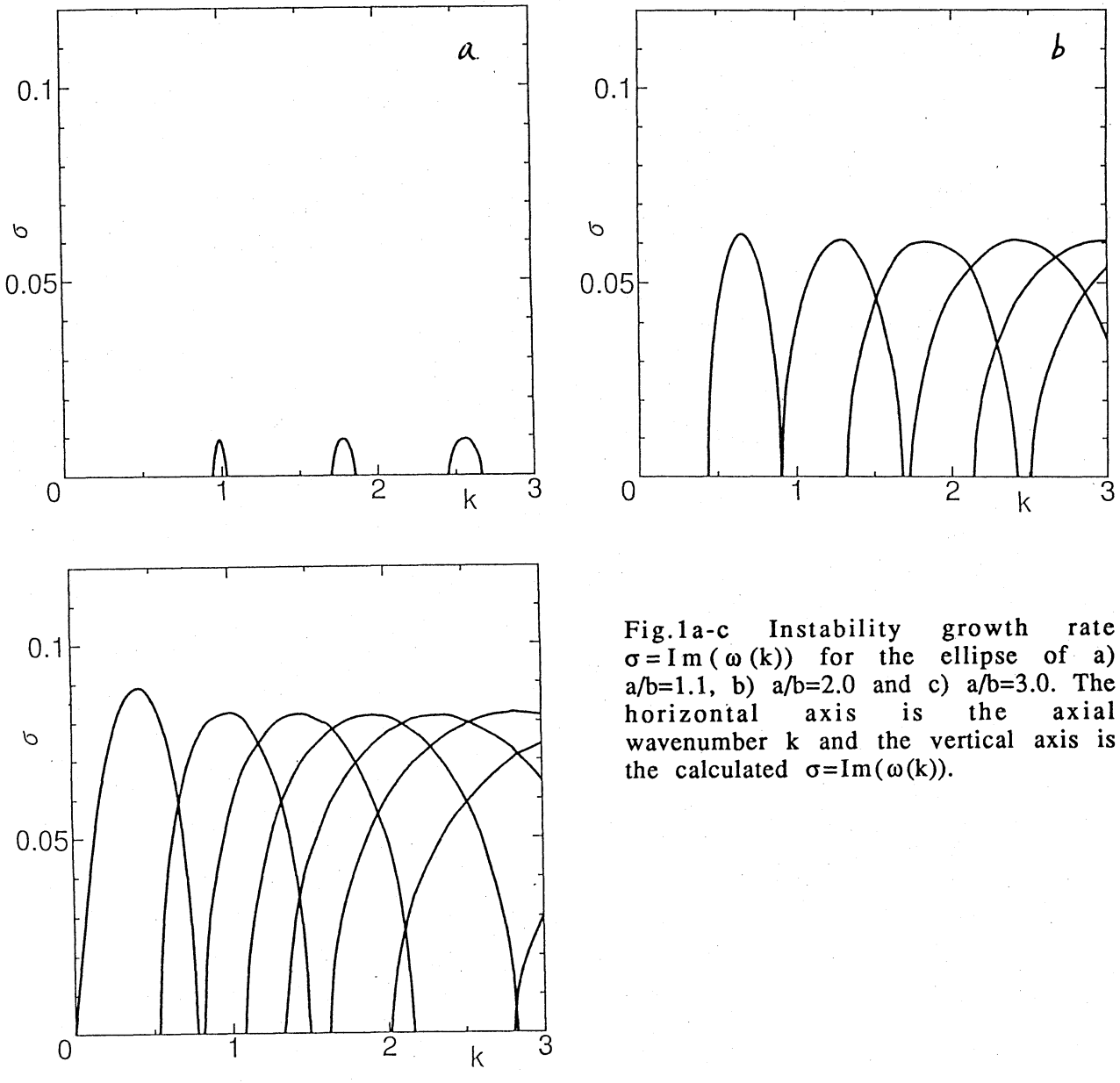

Fig.1a-c Instability growth rate $\sigma = Im(\omega(k))$ for the ellipse of a) a/b=1.1, b) a/b=2.0 and c) a/b=3.0. The horizontal axis is the axial wavenumber k and the vertical axis is the calculated $\sigma=Im(\omega(k))$.

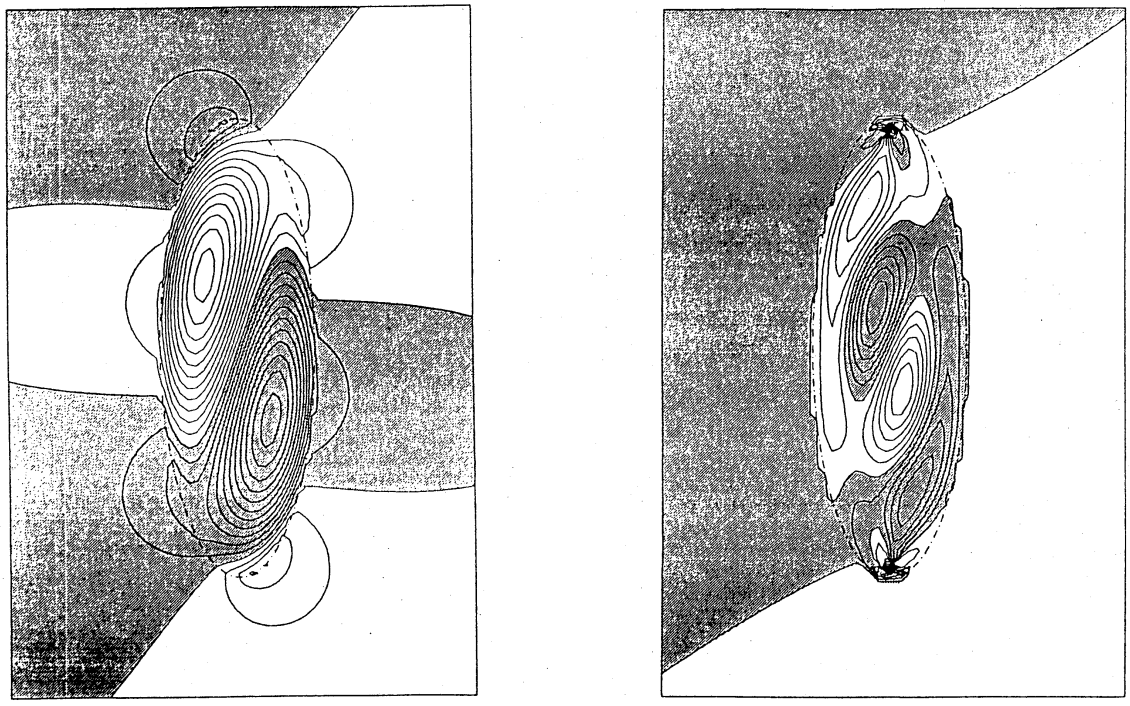

Fig.2a,b Axial velocity distributions in the x-y plane of a) the lowest eigenmode k=0.42 and b) the second eigenmode k=1.0, for a/b=3. The contour interval is arbitrary.

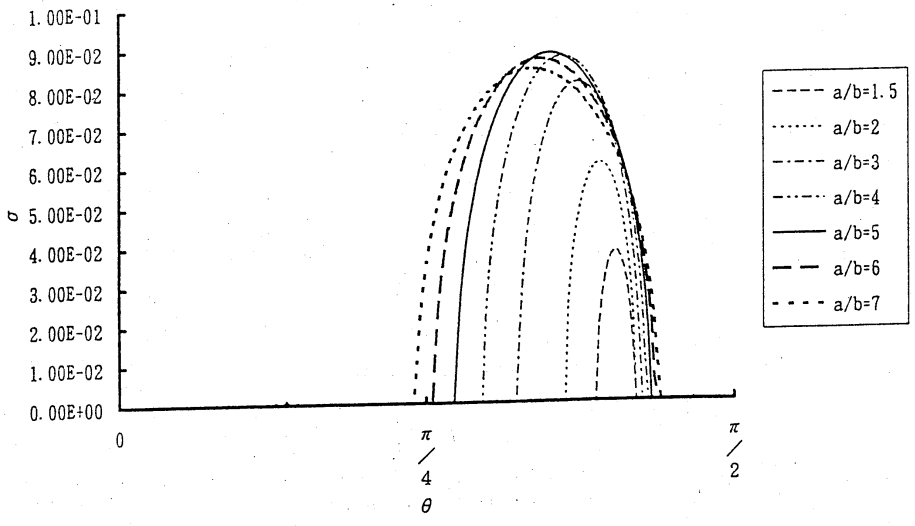

Fig. 3 Growth rate of the elliptical instability. The horizontal axis is the angle θ between the initial wavenumber and the z-axis. The vertical axis denotes the growth rate σ.

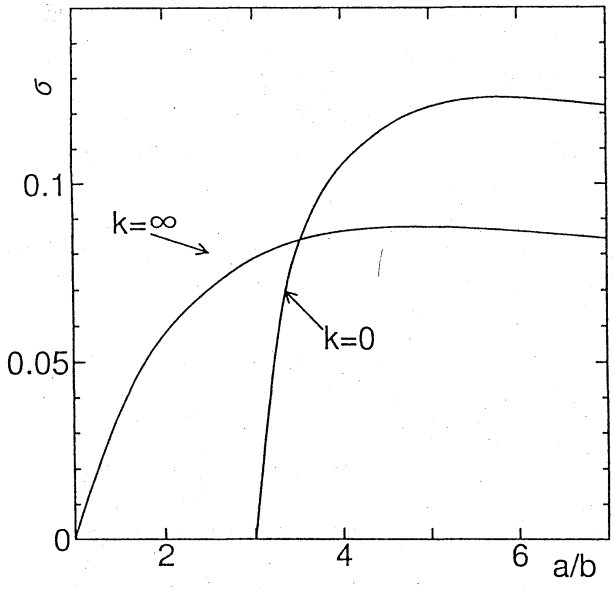

Fig. 4 Growth rate of the elliptical instability and the two-dimensional (m=3) instability of Kirchhoff's elliptic vortex. The horizontal axis is a/b. The vertical axis denotes the growth rate σ.

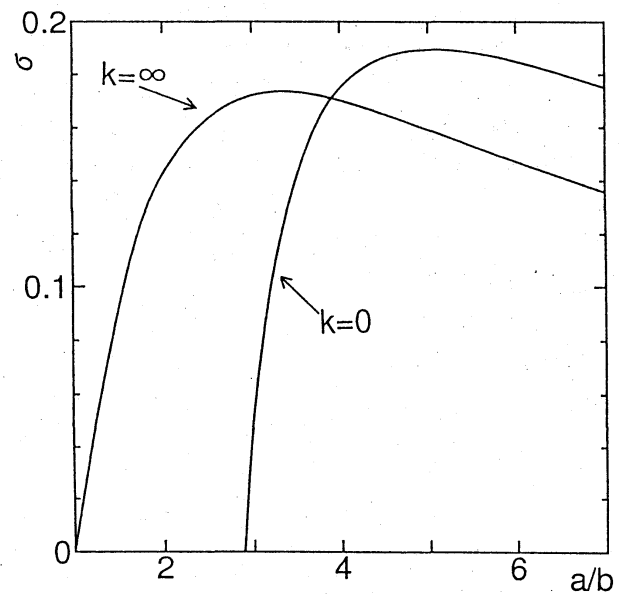

Fig. 5 Growth rate of the elliptical instability and the two-dimensional (m=2) instability of the Moore-Saffman elliptic vortex. The horizontal axis is a/b. The vertical axis denotes the growth rate σ.